

Review

# Relevant Parameters for the Mechanochemical Synthesis of Bimetallic Supported Catalysts

Maila Danielis <sup>1</sup>, Andrea Braga <sup>1,2</sup>, Núria J. Divins <sup>2</sup>, Jordi Llorca <sup>2</sup>, Alessandro Trovarelli <sup>1</sup>  
and Sara Colussi <sup>1,\*</sup>

<sup>1</sup> Dipartimento Politecnico, Università degli Studi di Udine, e INSTM, Via del Cotonificio 108, 33100 Udine, Italy

<sup>2</sup> Institute of Energy Technologies, Department of Chemical Engineering and Barcelona Research Center in Multiscale Science and Engineering, Universitat Politècnica de Catalunya, EEBE, Eduard Maristany 10-14, 08019 Barcelona, Spain

\* Correspondence: sara.colussi@uniud.it

**Abstract:** Mechanochemical synthesis for the preparation of bimetallic catalysts is gaining increasing interest, and in recent years, some important milestones have been reached. However, the complexity of mechanochemically prepared bimetallic supported catalysts still leaves many open questions that need a systematic approach to be solved. In this work, we summarize our experience of mechanochemically milling bimetallic catalysts, introducing some key parameters that should be taken into account, particularly the thermal stability and hydrophilicity of precursor salts, and the effect of the milling order, highlighting the differences with wet synthesis methods. Finally, we will provide some suggestions on the application of the design of experiments approach to the rationalization of the milling procedure for the preparation of supported bimetallic catalysts.

**Keywords:** dry milling; platinum; palladium; ceria; design of experiments



**Citation:** Danielis, M.; Braga, A.; Divins, N.J.; Llorca, J.; Trovarelli, A.; Colussi, S. Relevant Parameters for the Mechanochemical Synthesis of Bimetallic Supported Catalysts. *Crystals* **2023**, *13*, 1685. <https://doi.org/10.3390/cryst13121685>

Academic Editor: Bo Chen

Received: 17 November 2023

Revised: 5 December 2023

Accepted: 12 December 2023

Published: 14 December 2023



**Copyright:** © 2023 by the authors. Licensee MDPI, Basel, Switzerland. This article is an open access article distributed under the terms and conditions of the Creative Commons Attribution (CC BY) license (<https://creativecommons.org/licenses/by/4.0/>).

## 1. Introduction

Mechanochemical alloying is an old and well-known technique for the preparation of bimetallic compounds [1], but the milling of two (or more) metals to produce a catalytically active material is relatively recent. The first bimetallic catalytic formulations reported in the literature include, among the others, NiAl Raney catalysts [2], metallic carbides [3], electrocatalysts [4,5], and de-chlorination catalysts [6,7]. In these examples, metal powders were milled together, usually at high energy and for long times, to produce an active bimetallic compound that presented novel properties compared to those of single components. A different situation is one in which mechanochemical synthesis is exploited for the formation of metal alloys or bimetallic nanoparticles and their deposition on a support oxide, both occurring at the same time. It stems from the successful implementation of mechanochemical milling for the preparation of single metal-oxide electro- [8,9], photo- [10], and thermo-catalysts [11], a complex process in which a number of variables are involved, such as type of mill, energy, milling media, ball-to-powder ratio (BPR), powder hardness, metal-support interaction, etc. When this method is extended to the synthesis of bimetallic supported catalysts, an additional issue caused by the metal-metal interaction comes into the play, making a systematic approach difficult but highly desirable. So far, the number of research papers on supported bimetallic (thermo) catalysts obtained by ball milling is still quite limited [12–22]. However, some important elements have been highlighted. The simultaneous deposition of two metals can already be successfully obtained in short milling times and with relatively mild energy [13,19,21], but it strongly depends on the choice of the precursors and, possibly, on the support. Metal co-deposition is relatively easy with the appropriate conditions, but the formation of an alloy usually requires subsequent thermal treatments [13,20,21,23]. Interestingly, it has been found that energy-intensive thermal steps

can be overcome by longer milling times [11,14,24], even if this can lead to the contamination of the catalyst by the milling media. Regarding catalytic properties, the improvement of performance in terms of the activity, stability, and/or selectivity of bimetallic milled catalysts compared to analogous formulations obtained via other synthesis methods is widely reported. This has been ascribed in general to higher reducibility [13,21] and smaller particle size [16,17], indicating a stronger metal–support interaction, and to a different relative distribution of atomic species in milled vs. conventional catalysts [18,25]. Despite the setting of fundamental milestones, the complexity of mechanochemically prepared bimetallic supported catalysts still leaves many open questions. In this work, we introduce certain key parameters that should be taken into account when preparing bimetallic catalysts via mechanochemical milling, summarized in Figure 1. In particular, we will focus on the effect of precursor salts in terms of thermal stability and hydrophilicity on the final formulation and the effect of the milling order, and we will provide some suggestions regarding the application of the design of experimental approaches to the rationalization of the milling procedure for the preparation of supported bimetallic catalysts.

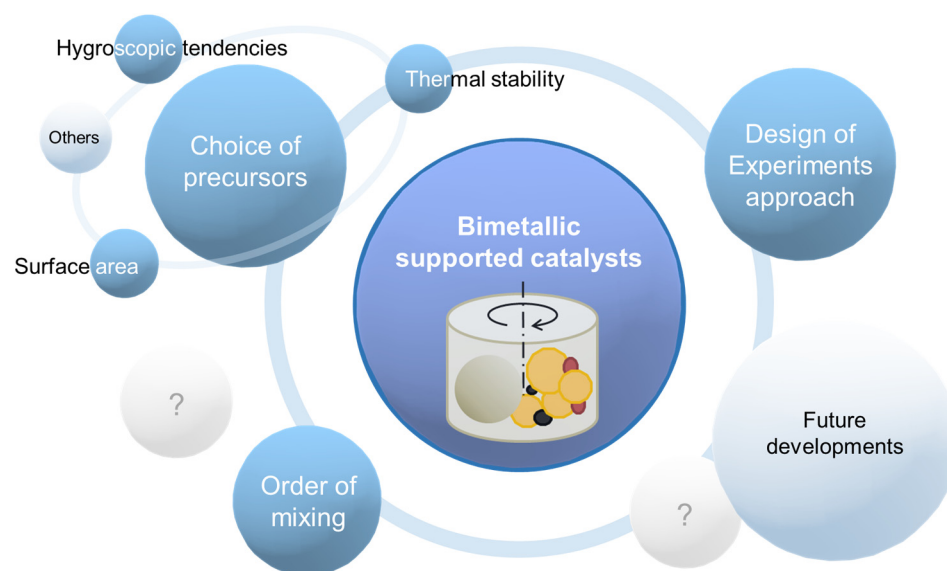


**Figure 1.** Relevant parameters and possible strategies for the preparation of bimetallic-supported catalysts. Question marks highlight the need for further research on unexplored parameters.

## 2. Choice of Precursors

As in traditional synthesis methods, one of the first parameters to be evaluated for bimetallic sample preparation is the type of metal precursor, be it metallic nanopowders, inorganic salts, or organic compounds. The combination of metals also requires particular attention. For example, if metallic platinum and palladium can be anchored on ceria after 15 min milling at 15 Hz in a vibratory micro-mill [13], the deposition of  $\text{PtO}_2$  and  $\text{Re}_2\text{O}_7$  on  $\text{TiO}_2$  is not completed after milling for 1 h at 150 rpm in a planetary mill [16], likely because metal oxides are harder compared to metals. In solution-precipitation methods, the main parameters relate to the solubility of the salt(s) and their characteristic pH needed for precipitation, affecting solvent choice and impregnation method [26]. However, in the dry milling procedure, the dissolution–precipitation steps are not required and factors such as temperature and concentration gradients or appropriate mixing are not a factor. Conversely, other properties of the metal precursors ought to be considered, such as:

- Thermal stability;
- Hygroscopic tendencies;
- Surface area, especially for metallic powders.

These variables should first be evaluated for each metal independently and then in combination with each other, identifying possible incompatibilities, if any. In the following, examples of each parameter effect are illustrated.

### 2.1. Thermal Stability

The thermal stability of precursor salts has been extensively studied in the past, and the characteristic boiling and evaporation temperatures of most salts are available in Safety Sheets. However, the decomposition behavior is not always reported in detail, and several studies only summarize, for example, the decomposition and volatilization tendencies of several metals, salts, or metal oxides [27–30]. While some have exploited these properties for wet-based syntheses to maximize metal dispersion [31,32], this might lead to metal loss when the dry milling synthesis is employed. The case of platinum is illustrative. Previous works on CeO<sub>2</sub>-supported Pd [33] and PdPt [13] catalysts have shown that dry milling is effective in inducing an intimate contact between the metal and the support oxide, resulting in a peculiar morphology with high activity and stability. In the monometallic example, the substitution of the metal (Pd black) precursor with the organic Pd acetate salt (Palladium(II)acetate, Pd(CH<sub>3</sub>COO)<sub>2</sub>, Sigma-Aldrich, Milan, Italy) led to a further increase in catalytic performance [34], while the addition of Pt in the metallic phase increased stability and resistance to water deactivation [13,25]. When attempting to merge the two advancements, Pt acetylacetonate (Platinum(II)acetylacetonate, Pt(O<sub>2</sub>C<sub>5</sub>H<sub>7</sub>)<sub>2</sub>, Sigma-Aldrich) was employed [35]. However, this salt tends to sublime, leading to Pt loss from the sample when heated [27,32]. This has been observed experimentally on a series of bimetallic PdPt/CeO<sub>2</sub> samples prepared starting from the organic precursors of Pt and Pd, summarized in Table 1. Samples were prepared by milling appropriate amounts of Pd acetate (Pdac) and Pt acetylacetonate (Ptacac) to reach a final metal loading of 1 wt%, following established procedures [13,34]. Pt and Pd content were measured using ICP-MS and thermogravimetric analysis (TGA). TGA was also performed on bare Ptacac salt, where full metal loss was observed (Figure 2a). Conversely, when a reducible oxide is used as support, it provides an anchoring point for some Pt atoms, which are not lost upon heating, as shown by data in Table 1 and Figure 2b. Indeed, weight profiles obtained by TGA were compared with the theoretical maximum and minimum weight expected in the opposite situations of total metal retention or full metal loss, %wt<sub>max</sub> and %wt<sub>min</sub>, respectively:

$$\%wt_{\max} = \frac{m_{\text{Pt}} + m_{\text{Pd}} + m_{\text{CeO}_2}}{m_{\text{in}}} \quad (1)$$

$$\%wt_{\min} = \frac{m_{\text{Pd}} + m_{\text{CeO}_2}}{m_{\text{in}}} \quad (2)$$

where *m* represents the final mass of Pt, Pd, and CeO<sub>2</sub> after thermal treatment, and *m*<sub>in</sub> is the initial mass of the fresh sample (CeO<sub>2</sub> + precursor salts).

**Table 1.** Weight and Pt content (wt%) measured by TGA and ICP-MS analysis on a series of bimetallic PtPd/CeO<sub>2</sub> milled (M) samples prepared from Pd acetate (Pdac) and Pt acetylacetonate (Ptacac) compared to theoretical calculated values.

Sample	%wt <sub>max</sub>	%wt <sub>min</sub>	%wt <sub>meas</sub>	%Pt <sub>nom</sub>	%Pt <sub>TGA</sub>	%Pt <sub>ICP</sub>
0.5Pt(acac)CeM	99.5	99.0	99.1	0.5	0.10	n.a.
0.5Pt(acac)0.5Pd(ac)CeM	98.9	98.5	98.7	0.5	0.25	0.20
0.5Pd(ac)0.5Pt(acac)CeM	98.9	98.5	98.7	0.5	0.25	n.a.
0.8Pt(acac)0.2Pd(ac)CeM	99.0	98.2	98.3	0.8	0.11	0.12

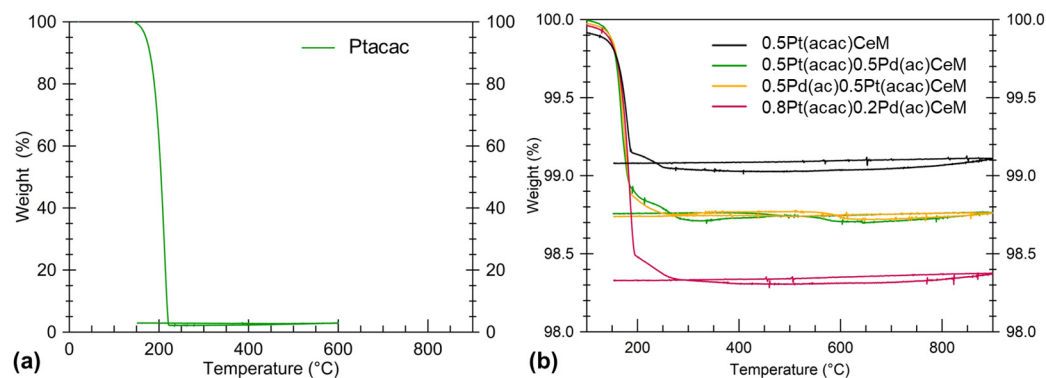


**Figure 2.** Weight profiles measured on (a) bare Pt acetylacetonate and (b) precursors salts milled (M) over  $\text{CeO}_2$ . TGA tests were carried out in a Q500 thermogravimetric balance (TA Instruments), heating at  $10\text{ }^\circ\text{C min}^{-1}$  up to  $900\text{ }^\circ\text{C}$  under  $\text{N}_2$ .

The presence of  $\text{CeO}_2$  clearly help to trap Pt atoms, as observed by calculated values on  $0.5\text{Pt}(\text{acac})\text{CeM}$  in Table 1, but Pd appears to be even more favorable, further promoting its stability by allowing a reduction in Pt loss from 80% to only 50%. This promotional effect is maintained regardless of the order of milling, whether Pd or Pt first ( $0.5\text{Pt}(\text{acac})0.5\text{Pd}(\text{ac})\text{CeM}$  or  $0.5\text{Pd}(\text{ac})0.5\text{Pt}(\text{acac})\text{CeM}$ , respectively), which suggests that the effectiveness of metal alloying, depending on reciprocal affinity [11,14], might be a significant barrier against metal evaporation. A similar effect was observed regarding the addition of silver acetylacetonate [36], where the stabilizing effect was attributed to weak interactions among chelates rather than alloying between the metals. A viable strategy to overcome the volatilization issue is to rely on Pt metal as precursor or, alternatively, to explore other inorganic salts. In the dry milling approach, there are no theoretical incompatibilities between precursors of a different nature, which would subsist when dissolution and precipitation are needed [26], as will be further illustrated in Section 4.

## 2.2. Hygroscopic Behavior of Precursor Salts

Some salts have a strong tendency to coordinate with ambient  $\text{H}_2\text{O}$ . While this does not usually represent a problem in solution-based syntheses, unless the stability of the metallic state is affected, it might strongly affect the mechano-chemical process. In fact, the coordinated water molecules act as “internal” solvent, thus affecting metal dispersion. Notable examples are nickel and calcium nitrates, which have been observed experimentally to retain a lot of water. When milled over ceria, the precursor salt might release the coordinated water, resulting in a semi-wet paste rather than a powdery product, as illustrated in Figure 3.

A similar phenomenon was observed with  $\text{Ca}(\text{NO}_3)_2 \cdot 6\text{H}_2\text{O}$ , used as promoter in  $\text{RuNi}/\text{CaO}/\text{CeO}_2\text{-Al}_2\text{O}_3$  formulations generally employed for integrated  $\text{CO}_2$  capture and conversion [37,38]. Herein, the same unpredictable uptake of atmospheric humidity was observed, leading to unsatisfactory results in terms of salt dispersion and thus requiring the controlled conditioning of the Ca precursor prior to materials synthesis. In fact, the performance of two samples prepared with the fresh calcium nitrate and with its counterpart aged under ambient conditions highlighted a loss of catalytic performance in standard  $\text{CO}_2$  capture and  $\text{H}_2$  reduction, as summarized in Figure 4a. In fact, both the absolute  $\text{CO}$  production during  $\text{H}_2$  exposure and the production during  $\text{CO}_2$  capture were affected, suggesting a loss in adsorptive sites and, consequently, decreased reactivity [37]. The effect of the increased humidity of the precursor salt was also followed by thermogravimetric analysis. The weight loss profiles, reported in Figure 4b, clearly highlight the higher amount of hydration on the “aged” sample, i.e., the one prepared with humid calcium nitrate, where an additional 2.7 wt% loss below  $120\text{ }^\circ\text{C}$  is observed compared to the fresh sample, due to adsorbed water. Moreover, the decomposition of the supported salts (Ni and Ru, in addition to Ca) is delayed, as observed by the weight derivative signal at  $300\text{ }^\circ\text{C}$ .



This might be due to the weaker contact between the nickel and ruthenium salts and the calcium nitrate, further corroborating the observed loss in performance. In conclusion, the uncontrolled hydration of the precursors might lead to the insufficient dispersion of the metal, inefficient milling, and reproducibility inconsistencies.



**Figure 3.** Pictures of Ni/CeO<sub>2</sub> samples milled with H<sub>2</sub>O-rich precursor salts. The same synthesis of Ni/CeO<sub>2</sub> was carried out using Ni(NO<sub>3</sub>)<sub>2</sub>·6H<sub>2</sub>O, a heavily hygroscopic salt, and ceria powders; the preparation was repeated with the same procedure on different days characterized by different levels of relative atmospheric humidity. The results varied on a daily basis as different levels of humidity were present; during the most humid days, the amount of H<sub>2</sub>O adsorbed by the salt was enough to create a wet layer and separate the finely dispersed Ni nitrate salts from the ceria.

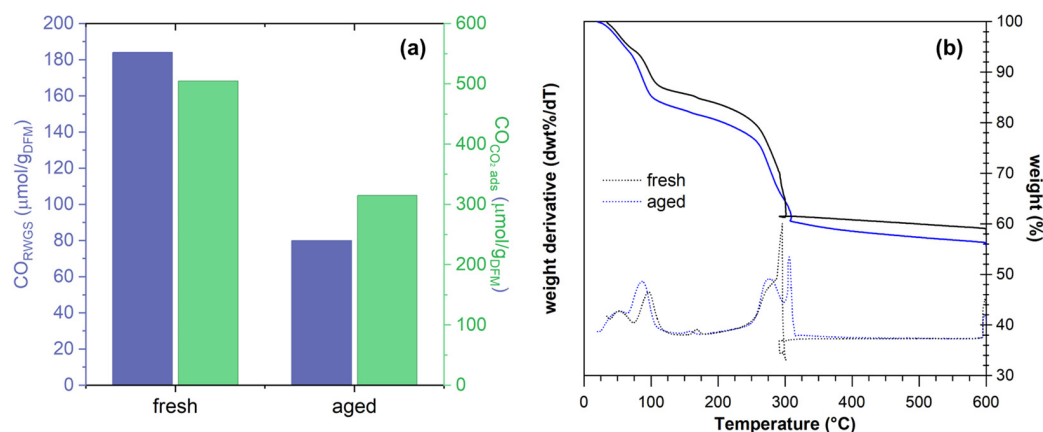


**Figure 4.** Comparison of two NiRu/CaO/CeO<sub>2</sub>-Al<sub>2</sub>O<sub>3</sub> samples prepared via milling using fresh or aged (humid) calcium nitrate: (a) CO production during CO<sub>2</sub> capture (10 vol% CO<sub>2</sub>/N<sub>2</sub>) and H<sub>2</sub> reduction (10% H<sub>2</sub>/N<sub>2</sub>) looping tests carried out at 650 °C (WHSV = 12,000 mL g<sub>DFM</sub><sup>-1</sup> h<sup>-1</sup>); (b) weight profiles measured during TGA experiments in air, heating at 10 °C min<sup>-1</sup> up to 600 °C.

### 2.3. Surface Area

The surface area of precursor powders is usually considered only with regard to the support oxide, whose obvious role is to ensure the optimal dispersion of the active metal phase, and thus, a high surface area is favorable. Nonetheless, the available surface of the metallic phase, when the dry milling procedure is carried out, starting from metallic precursors, likely plays a non-negligible role in favoring metal–support interactions. Examples of

surface area values for selected metal powders are reported in Table 2, together with the nominal particle size provided by the supplier.

**Table 2.** Surface area and nominal particle size values of metallic nanopowders.

Sample	Provider	Particle Size	BET S.A. (m <sup>2</sup> /g) <sup>1</sup>
Ru black	Strem Chemicals <sup>2</sup>	n.a.	51
Pd black	Sigma-Aldrich <sup>3</sup>	10 μm	40
Pt black	Sigma-Aldrich	<20 μm	33
Ni nanopowder	Sigma-Aldrich	<20 μm	<1
Cu	Sigma-Aldrich	<425 μm	6
PdO	Sigma-Aldrich	<10 μm	74

<sup>1</sup> Measured by BET analysis of N<sub>2</sub> isotherms at 77 K in a Micromeritics Tristar 2000 instrument; <sup>2</sup> Bischheim, France; <sup>3</sup> Milan, Italy.

This factor is arguably less important than chemical affinity, as shown by the example of PdO particles: despite the high surface area, the palladium oxide powders do not react during milling and lead to an unsatisfactory dispersion over the ceria surface [33]. However, generally metals with lower available surface areas showed a worse dispersion when milled on ceria, resulting in a decreased catalytic activity when compared to their counterpart prepared via traditional wet-based impregnation synthesis (IW) (Figure 5a–c). This unfavorable interaction can be mitigated by the addition of a co-metal, such as Pd, which could provide a source of affinity and enhance the dispersion of the bimetallic phase [33,39,40], further resulting in improved catalytic performance, as highlighted in Figure 5d,e.

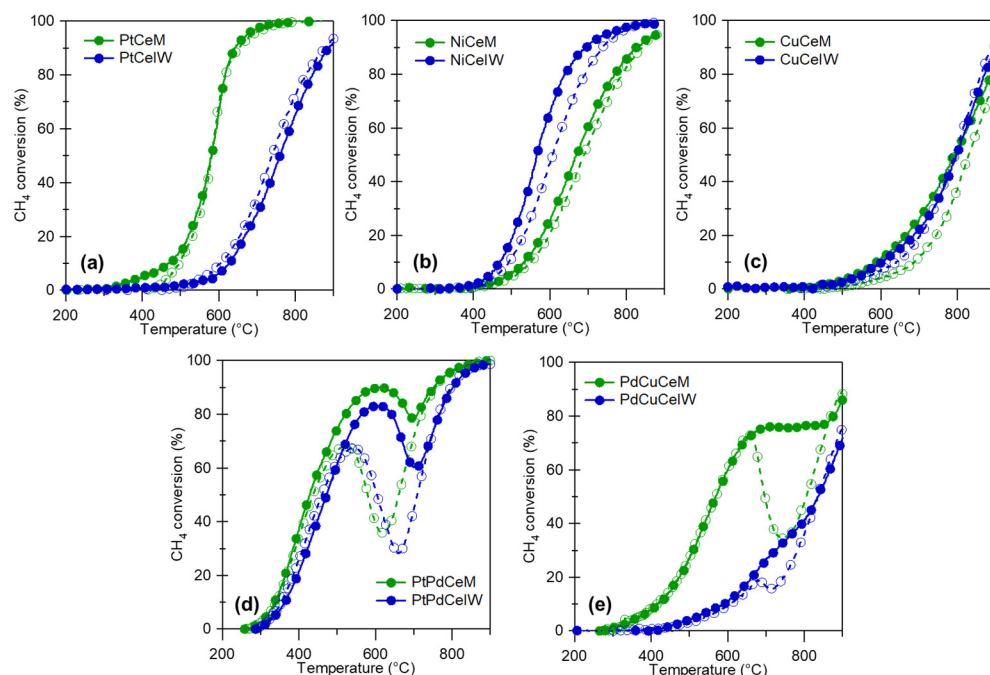


**Figure 5.** Methane oxidation activity in transient light off tests on (a) 1 wt%Pt/CeO<sub>2</sub>, (b) 4 wt%Ni/CeO<sub>2</sub>, and (c) 1wt%Cu/CeO<sub>2</sub> milled (M) and conventional (IW) catalysts. Comparison with bimetallic formulations for (d) PdPt/CeO<sub>2</sub> and (e) PdCu/CeO<sub>2</sub> samples. Gas feed: 0.5%CH<sub>4</sub>; 2%O<sub>2</sub> in He; GHSV = 180,000 h<sup>-1</sup>; heating (solid) and cooling (dashed) ramps, 10 °C min<sup>-1</sup>.

#### 2.4. Other Parameters

Possibly, additional factors might play a role in the effectiveness of the mechanochemical synthesis for supported bimetallic catalysts. In fact, much uncertainty still persists with regard to the chemical reactions induced by milling, requiring additional experimental

and theoretical studies. As an example, the hardness of powders precursors might play a role in the successful preparation of supported metal catalysts [13,33], yet their relative importance, e.g., compared to some of the parameters elucidated above, is yet to be understood. Moreover, data regarding hardness properties of nanopowders, called nano- or microhardness [41,42], is still largely lacking for materials commonly used for catalytic applications, thus inhibiting correlation with this parameter when analyzing the dry milling processes of metal nanopowders. Recent reports on other classes of materials [43] will most likely promote such an investigation in the near future.

In synthesis, when evaluating the best precursors for bimetallic samples prepared by milling, the following parameters should be considered:

- Intrinsic volatility of the precursor salt might cause metal loss;
- Different treatment atmospheres or support oxides affect volatility;
- Heavy hydration of precursor salts leads to inhomogeneous and/or irreproducible results;
- When using metallic nanopowders, high surface area usually promotes chemical interaction;
- Hardness values could play an additional role, facilitating the milling of soft materials.

### 3. Order of Mixing

The order of metal addition to the metal–support combination plays a key role in determining the overall efficiency of the synthesis process. This has been explicitly proven in PtPd/CeO<sub>2</sub> systems [13,25], where two samples were prepared by milling Pd and Pt powders in subsequent steps (denoted as PtPdCeM and PdPtCeM, where the metal close to CeO<sub>2</sub> is milled first and M indicates the synthesis method). The PtPdCeM catalyst benefits from the unique Pd–CeO<sub>2</sub> interaction [33], and indeed, HRTEM evidence shows the formation of an amorphous shell covering Pt and PtPd entities [13]. This amorphous shell, containing Pd–O–Ce units, has been identified as being responsible for the outstanding activity of Pd/CeO<sub>2</sub> milled catalysts [33]. Conversely, when the order of milling is inverted (i.e., first Pt with CeO<sub>2</sub> followed by the milling of Pd), on PdPtCeM high-angle annular dark-field (HAADF) scanning transmission electron microscopy (STEM), coupled with energy dispersive X-ray (EDX) analysis, revealed the presence of isolated Pt and Pd clusters without any amorphous layers [13]. The different configurations result in a higher amount of “free” metals, i.e., not interacting with each other [25], leading to worse performance under transient light-off and stability experiments, as reported in Figure 6. The promotional effect of the Pd–CeO<sub>2</sub> interaction was also observed on catalytic samples prepared by milling Pd acetate and Pt acetylacetonate salts, where, despite no quantitative effect on the Pt loss induced by the organic salt volatility, the presence of pre-milled Pdac on CeO<sub>2</sub> would improve the catalytic activity of Pt retained on the final catalyst formulation (Figure 6b) [35].

Similar results were obtained for other metallic systems, where Pt was substituted by either Sn or Cu in PdPt/CeO<sub>2</sub> formulations [39,40]. On PdSn formulations, once again performing a first milling step with Pd and CeO<sub>2</sub> led to higher activity compared to milling Sn first, as demonstrated by reference methane oxidation activity tests in Figure S1a (see the Supplementary Materials). Conversely, adding Sn in the first milling step led to a slight decrease in performance, yet still outperforming the reference SnPdCeIW reference sample. Here, it can be hypothesized that the ductility of the Sn metal and its strong affinity with CeO<sub>2</sub> [44] concur in improving tin dispersion over ceria by milling compared to the conventional IW synthesis. However, by bonding with, or, possibly, within the CeO<sub>2</sub> support, Sn reduces the Pd–Ce interaction, thus decreasing its CH<sub>4</sub> activation performance under reaction conditions. Interestingly, PdCu systems displayed no significant sensitivity in terms of the order of metal addition, as shown in Figure S1b. Milling in reciprocal sequential order or co-milling the metals together (denoted as (PdCu)CeM) resulted in comparable methane oxidation reactivity. This might be due to the weak affinity between Pd and Cu and Cu and Ce.

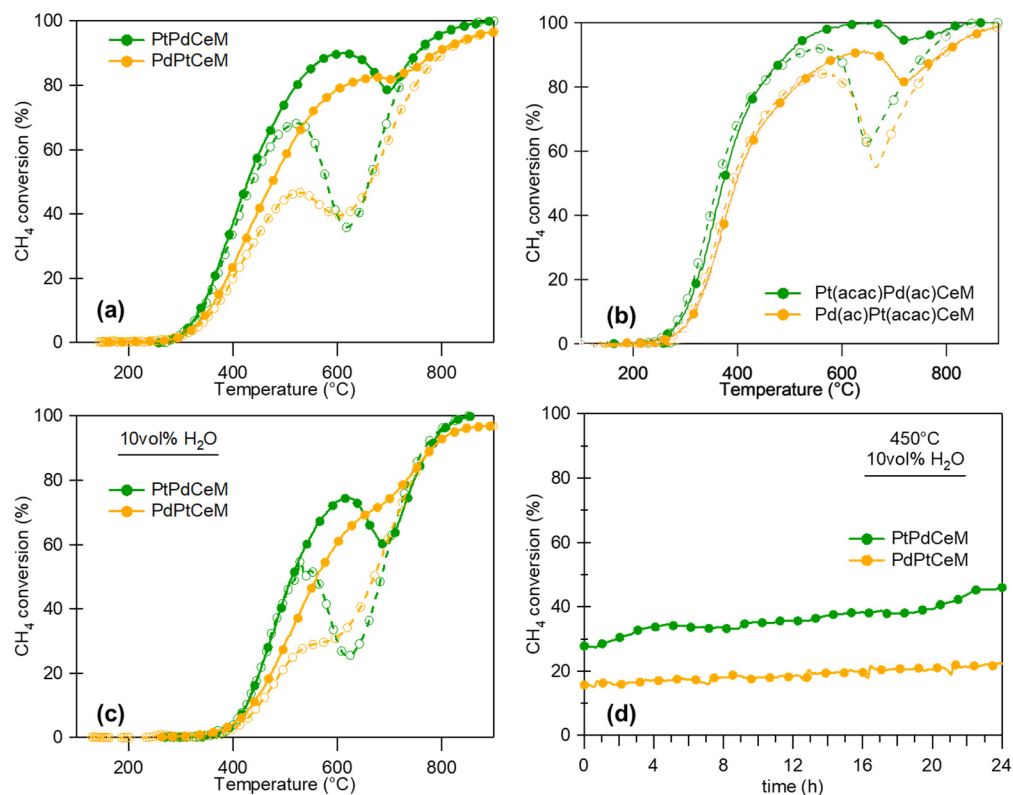


**Figure 6.** Methane oxidation activity in (a)–(c) transient light off tests and (d) stability tests for PdPtCeM and PtPdCeM milled samples (0.5 wt%Pd, 0.5 wt%Pt). (a,c,d) Samples prepared from metallic powders; (b) samples from organic salts. (a,b) Gas feed: 0.5%CH<sub>4</sub>, 2%O<sub>2</sub> in He; (c,d): 0.5%CH<sub>4</sub>, 2%O<sub>2</sub>, 10%H<sub>2</sub>O in He. GHSV = 180,000 h<sup>-1</sup>; heating (solid) and cooling (dashed) ramps, 10 °C min<sup>-1</sup>.

In sum:

- The sequential vs. simultaneous milling of metals over the support might affect the formation of bimetallic nanoparticles;
- By affecting either their alloying and/or their dispersion;
- The reciprocal affinity between metals, or between each metal and the support, should be considered;
- Following Le Chatelier's principle, too strong and too weak an affinity will likely lead to unsatisfactory results.

#### 4. DOE Approach

It is evident from the previous paragraphs that there is an interplay between the many synthesis parameters and the chemical nature of the precursors. Obtaining the desired material structure and catalytic properties requires finding the right set of parameters for material preparation. The optimization of a synthesis procedure usually requires a large amount of work, and this is especially true while investigating the many parameters involved in the mechanochemical preparation of catalysts. Consequently, there has been a growing interest in the optimization of such experimental campaigns [45,46]. In this paragraph, the use of the design of experiment (DOE) approach for the mechanochemical preparation of PtNi/CeO<sub>2</sub> catalysts for the steam reforming of methane is reported.

Commonly, studying and optimizing a problem defined by many parameters is done by selecting an initial set of parameters as the starting experimental condition and proceeding by varying one variable at a time (the so-called OVAT approach [47]). Each parameter is changed while keeping the others fixed, observing its effects on the system. The study continues after finding the best results by varying another parameter from this point, and another parameter is then modified while fixing the others. This process is repeated for



each parameter until an optimized result is reached after studying all the parameters. While this is the common practice and the most intuitive way of performing experiments, this approach is characterized by several limitations [47,48]. The final result is often strongly influenced by the initial set of parameters: varying one variable at a time allows for finding the optimal result for a single parameter in a specific combination with the others, and the following optimal results rely on the previous experimental runs. In this regard, interactions between the parameters are not determined, as the various parameters are not tested for all the different combinations. Another aspect to be considered is that, in principle, the total number of experiments is not known in advance, as it is difficult to exactly predict how many experiments are needed to reach a desired result.

Another approach to study complex problems is the so-called design of experiment methodology [47,49,50], which is a methodology based on the statistical design of experiments and the analysis of their results. Briefly, the DOE approach relies on the simultaneous and systematic variation of all the parameters involved in the study to obtain the highest amount of information while keeping the number of experiments low. Based on the various designs available, the statistical analysis of the results can provide several pieces of information, i.e., the identification of the most important parameters in a screening experiment, the effect and interactions of all the parameters studied, or the precise mathematical model to identify the real optimal set of parameters for the desired properties.

Studying a problem or exploring a system with a DOE approach requires the identification of the parameters which can influence the results or the parameters of interest to be studied, and to define the experimental domain, which is the space generated by the different parameters and their possible values. Based on the objective of a study, different types of designs are available with a specific combination of experimental parameters and a given number of experiments. After choosing the parameters to be studied, their ranges, and the right balance between the number of experiments and the information to be obtained, an experimental design is created, and the plan is systematically executed. All the results are collected and included in the statistical analysis to obtain the desired information.

The DOE approach has many advantages over the classical OVAT methodology. The final results are not influenced by the previous experiments, as each experimental run is performed independently. This also means that the number of experiments is known in advance, allowing for more efficient time planning and resource optimization. Often, the designs are performed in a random manner to avoid systematic errors and avoid the influence of external effects. The experimental domain is explored more efficiently and in a broader manner, as all the values and the combinations of the different parameters are tested, not limiting the investigation around the best values observed from the previous runs. This implies that the quality and the amount of knowledge of the system is higher, as the whole system is explored by obtaining a more general view on the effects of the various parameters. This is usually achieved with a lower number of experiments compared with the OVAT approach.

Herein, an illustrative example of the application of a Fractional Factorial Design for the preparation of PtNi/CeO<sub>2</sub> catalysts is reported. For these materials, the most important factors for high catalytic performances are a small size of the active phase, namely Pt and Ni nanoparticles, and a high degree of interaction between Pt, Ni, and CeO<sub>2</sub> [51–53]. The mechanochemical procedure to prepare the series of PtNi/CeO<sub>2</sub> catalysts was based on the FRITSCH Mini-Mill Pulverisette 23, and three milling parameters were investigated: the milling frequency, the milling time, and the ball-to-powder ratio (BPR). The objective of the screening study was to quickly identify the milling parameter with the strongest influence on the NiO particle size and the methane conversion at 700 °C, and to obtain a set of samples for efficiently exploring the effect of varying the milling intensity. The catalytic materials were prepared with nominal metal loadings of 0.9 wt.% Pt and 8.1 wt.% Ni on CeO<sub>2</sub> (25 m<sup>2</sup>/g, calcined at 950 °C for 5 h in air) by mixing together appropriate amounts of Ni acetate, Pt(NH<sub>3</sub>)<sub>2</sub>(NO<sub>3</sub>)<sub>4</sub>, and the CeO<sub>2</sub> powders in a 15 mL ZrO<sub>2</sub> jar with a single 10 g ZrO<sub>2</sub> ball. The milled powders were then kept at 120 °C for 12 h and calcined at 400 °C

for 4 in air to decompose the metal precursors. Pt and Ni precursors were chosen based on thermal stability and hygroscopic properties, as illustrated in Section 2.

A Fractional Factorial Design with a central point was used to efficiently explore the possible combinations of the three milling parameters (frequency, time, BPR) and to find the best parameters for the catalyst preparation, keeping the number of samples as low as possible [49]. A representative scheme is reported in Figure S2. In addition, this design allows us to obtain useful information about the direct effect of each parameter on the NiO particle size and the catalytic activity, identifying which parameter is the most influential and the general trends. The sample names and the synthesis parameters are shown in Table 3, reported with increasing milling intensity order. The experimental plan was created with the DOE module included in Minitab19.

**Table 3.** Sample names, catalytic performance, and values of the three milling parameters studied with the Fractional Factorial design of experiment.

Sample	Frequency (Hz)	Milling Time (min)	BPR
1-PtNiCe(−−+)	15	5	20
2-PtNiCe(−++)	15	45	5
3-PtNiCe(+−−)	50	5	5
4-PtNiCe(000)	32.5	25	12.5
5-PtNiCe(+++)	50	45	20

This set of five samples contains enough combinations of the different parameters which were tested twice, at the low and high parameter values. The sample 4-PtNiCe(000) is called the central point, and it was prepared with a set of parameters lying in the center of the three-dimensional experimental domain. Its function is to qualitatively evaluate the non-linearity of the system properties.

The samples were characterized via X-ray diffractometry (XRD), temperature programmed reduction tests under H<sub>2</sub> (H<sub>2</sub>-TPR), and Raman spectroscopy to assess their structures and the interactions between the various components. All the diffractograms showed the CeO<sub>2</sub> XRD pattern with no differences in the peak widths and in the relative peak intensities, indicating that the wide range of milling parameters tested did not influence the bulk structure of CeO<sub>2</sub>. Besides the CeO<sub>2</sub> XRD pattern, Ni, Pt, and NiO reflections were observed; the particle size of both Pt and NiO decreased with increasing milling intensity, indicating a better dispersion of the active metal phase on the surface of ceria. In Table S1, the crystallite size of NiO estimated using the Scherrer equation is reported. The Raman spectra showed the main CeO<sub>2</sub> peak centered at 464 cm<sup>−1</sup> relative to the F<sub>2g</sub> bulk vibration [54]; the position and width of this peak was not modified with increasing milling intensity, meaning that the bulk structure of ceria was not affected. By increasing the milling intensity, the H<sub>2</sub>-TPR profiles suggested that an increased interaction between Pt and Ni species is achieved, that the Pt-Ni alloy is formed upon reduction at 350–400 °C, and that a stronger interaction with the support material is obtained. Further confirmation of the increased interaction between the different components was obtained from the Raman spectra. By increasing the milling intensity, a rapid increase in the Raman signal at 500–600 cm<sup>−1</sup> was observed (see Table S1), which is associated with CeO<sub>2</sub> defects and oxygen vacancies and is typically found in Ni/CeO<sub>2</sub> materials [55]. Table S1 shows the methane conversion during the methane steam reforming reaction at 700 °C. There is a clear trend between the milling intensity and the catalytic activity in the range of the investigated milling parameters. Smaller NiO and Pt particle sizes, stronger interactions with CeO<sub>2</sub>, and the easier formation of the Pt-Ni alloy are the main factors of the increased catalytic activity.

The last part of a DOE experiment is the statistical analysis of the results. Using the Minitab19 DOE module, the NiO particle size and the methane conversion at 700 °C were used to measure the effect of each milling parameter on these two properties. Equations (3) and (4) show the effect of each variable on the two properties: the higher the coefficient, the stronger

is the effect. The effect of each variable on the two properties is also shown graphically in Figure 7; each point represents the average value of the given property at different parameter values. The steeper the line, the stronger the parameter-changing effect. The red dot represents the value related to 4-PtNiCe(000). It is evident that the most important parameter is the milling frequency, which is directly related to both an increasing number of impacts and the kinetic energy of each impact. The second most important parameter is the milling time, although a definitive conclusion cannot be drawn as the central point suggests that a more complex relationship between time and ball-to-powder ratio (BPR) might exist.

$$\text{NiO NP size (nm)} = 26.27 - 0.23 \times \text{frequency} + 0.0062 \times \text{Time} - 0.19 \times \text{BPR} \quad (3)$$

$$X_{\text{CH}_4@700\text{ }^\circ\text{C}} = 3.65 + 1.10 \times \text{Frequency} + 0.58 \times \text{Time} + 0.010 \times \text{BPR} \quad (4)$$

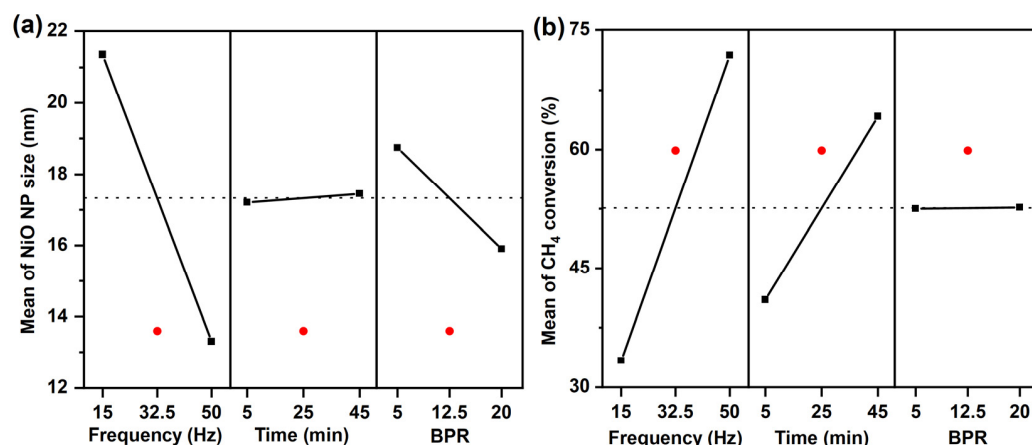


**Figure 7.** Effect of each milling parameters on (a) the NiO crystallite size and (b) the methane conversion at 700 °C ( $F/W = 202,500 \text{ mL/g}_{\text{cat}} \text{ h}$ , steam-to-carbon ratio = 2). Each black point represents the mean value of the NiO particle size or the methane conversion obtained from all the samples prepared with that parameter; for example, the average value of methane conversion at 50 Hz is 71.9%, obtained from the methane conversion of samples 3-PtNiCe(+−−) and 5-PtNiCe(+++) which displayed, respectively, 60.2 and 83.5% CH<sub>4</sub> conversion. The red dot corresponds to the value of sample 4-PtNiCe(000).

These results were obtained with just five samples and are useful for the further study and development of the PtNi/CeO<sub>2</sub> catalytic system with the mechanochemistry: a high-energy regime is required to induce the desired interactions between Pt, Ni, and CeO<sub>2</sub>, while a lower milling time and ball-to-powder ratio (BPR) might be enough to obtain an active catalyst with a larger amount of catalyst produced, as more sample can be prepared in a shorter amount of time. From this point, the fractional design could be augmented to a full factorial design by adding four more samples, and thus, more precise and complete information about the parameters and their interactions could be obtained [49]. Other options could be exploring higher milling intensity regimes to extend the energy range and observe if further enhancements are obtained, as well as extending the milling times to see whether higher methane conversion rates are obtained.

## 5. Comparison with Wet Methods

In the above paragraphs, the feasibility of the mechano-chemical synthesis for the preparation of bimetallic supported catalysts was outlined. Despite the characteristic advantages of the dry milling method, such as reduced solvent utilization, thermal treatments, and waste generation [56,57], the appropriate tuning of milling parameters might be hindered by the multiple, interconnected factors affecting materials preparation, some of which were highlighted previously, and that strongly depend also on the catalytic formulation and application of choice. Consequently, the application of the mechanochemical synthesis

at the industrial level is not as straightforward as desired. Multiple recent studies are contributing to the scaling up of milling process parameters by modeling [58–60] and by showing promising results in terms of the preparation of single-atom catalytic materials [61] and even of structured catalysts [62]. Yet, additional factors such as capital and operational costs (CAPEX and OPEX, respectively) are considered at an industrial level before abandoning established catalyst synthesis processes, such as wet impregnation methods, in favor of novel routes. Therefore, despite successful literature reports, additional studies will be required to hasten technological transfer at the commercial level. A comparison of the two synthesis methods is reported in Table 4.

**Table 4.** Comparison between dry milling and wet impregnation methods for the preparation of metal-supported catalysts.

	Mechanochemical Synthesis	Wet Synthesis
Use of solvents	no	necessary
Thermal treatments	maybe	necessary
Order of metal addition	relevant	maybe relevant
Choice of precursors	relevant	relevant
Contamination from synthesis media	possible	unlikely
Versatility	limited *	yes
Scalability	yes	yes
Industrial readiness level	In progress	Full application

\* based on current experimental data.

## 6. Conclusions

In this paper, we overviewed the challenges presented by the dry mechano-chemical preparation of supported bimetallic catalysts. In particular, factors such as thermal stability, hygroscopic tendencies, and surface area of metal precursors, among others, have to be considered in addition to their relative affinity to ensure the effectiveness of the milling method and the intimate contact and alloying of supported metals. The order of mixing is also reported as a key factor affecting the successful dispersion of both metals, sometimes leading to significant differences in the final bimetallic systems obtained by dry milling. Naturally, these factors should be evaluated in combination with the usual milling parameters, such as frequency, time, ball-to-powder ratio, and type of milling media. Nonetheless, much uncertainty still exists in the field on how mechanically induced reactions and processes occur; thus, different factors might play a role in systems other than the metals supported on redox oxides discussed in this paper. Additional investigation is certainly necessary to increase the available knowledge on mechano-chemical processes.

The complexity of the system can lead to time-consuming experimental investigation. In fact, as reported in Section 4, the most common method of conducting research is by varying one variable at a time (OVAT). Exploring all the combinations of the different parameters is a time and resource-expensive task, and it can be difficult to clearly identify which parameter (or parameters) is responsible for the outcome. Moreover, the total number of experiments is unpredictable, usually higher than statistical methods, and strongly depends on the initial parameters of choice, and optimal results are not guaranteed [47]. A statistical approach such as the design of experiment strategy can be a viable solution to hasten the experimental screening of bimetallic catalysts, as well as to provide deeper insights into the effect of each parameter on the supported bimetallic catalytic system under investigation. In fact, the DOE approach allows for the identification of the minimum number of experiments needed for the experimental evaluation of defined parameters by setting a defined number of initial tests, which can ultimately lead to the statistical analysis of the results that contain information about all the parameters and their direct and/or combined effect on the system.

## 7. Patents

Significant findings have been patented by A. Trovarelli, S. Colussi, M. Danielis, J. Llorca, and A. Toso, in “Catalysts based on Pd/CeO<sub>2</sub> and preparation method thereof”. Patent numbers IT201700070360A—23 June 2017, EP3651898A1, WO2018235032A1.

**Supplementary Materials:** The following supporting information can be downloaded at: <https://www.mdpi.com/article/10.3390/cryst13121685/s1>, Figure S1: Methane oxidation activity of (a) PdSn/CeO<sub>2</sub> and (b) PdCu/CeO<sub>2</sub> catalysts; Figure S2: Graphical representation of the 3D space generated by the three variables, including the central point; Table S1: Methane conversion at 700 °C, NiO crystallite size inferred by XRD measurements, and normalized Raman intensity of the signal at 570 cm<sup>-1</sup> (typical of Ni-O-Ce bonds and oxygen vacancies) for the samples prepared with the Fractional Factorial design.

**Author Contributions:** Conceptualization, S.C. and M.D.; investigation, data curation, methodology, formal analysis, M.D. and A.B.; validation, S.C. and N.J.D.; writing—original draft preparation, S.C., M.D. and A.B.; visualization, M.D.; supervision, S.C., N.J.D., J.L. and A.T.; writing—review and editing, project administration, funding acquisition, J.L. and A.T. All authors have read and agreed to the published version of the manuscript.

**Funding:** This research was funded by the European Union Next-Generation EU (Piano Nazionale di Ripresa e Resilienza (PNRR)—Missione 4 Componente 2, Investimento 1.5—D.D. 1058 23/06/2022, ECS00000043); by MICINN/FEDER, grant number PID2021-124572OB-C31; and by Generalitat de Catalunya, grant number GC 2021 SGR 01061.

**Data Availability Statement:** The data presented in this study are available on request from the corresponding author. The data are not publicly available due to ongoing research on some topics.

**Acknowledgments:** Contribution from Chiara Pascoli, Lorenzo Mongiat, and Andrea Mussio is kindly acknowledged. M.D. is grateful for funding under the REACT EU Italian PON 2014–2020 Program—Action IV.4—Innovation (DM 1062, 10 August 2021). A.B. and A.T. acknowledge the Interconnected Nord-Est Innovation Ecosystem (iNEST) under the European Union Next-Generation EU (Piano Nazionale di Ripresa e Resilienza (PNRR)—Missione 4 Componente 2, Investimento 1.5—D.D. 1058 23 June 2022, ECS00000043). A.B. is grateful to the European Union’s H2020 research and innovation program under the Marie Skłodowska-Curie grant agreement no. 813748. J.L. is a Serra Hünter Fellow and is grateful to the ICREA Academia program.

**Conflicts of Interest:** The authors declare no conflict of interest.

## References

1. Lin, I.J.; Nadiv, S. Review of the Phase Transformation and Synthesis of Inorganic Solids Obtained by Mechanical Treatment (Mechanochemical Reactions). *Mater. Sci. Eng.* **1979**, *39*, 193–209. [[CrossRef](#)]
2. Fasman, A.B.; Mikhailenko, S.D.; Kalinina, O.T.; Ivanov, E.Y.; Golubkova, G.V. Synthesis and Regeneration of Raney Catalysts by Mechanochemical Methods. In *Preparation of Catalysts V*; Poncelet, G., Jacobs, P.A., Grange, P., Delmon, B., Eds.; Elsevier Science Publishers B.V.: Amsterdam, The Netherlands, 1991; pp. 591–600. ISBN 2013206534.
3. Alves, A.M.; Rosenthal, R.; Teixeira Da Silva, V.L.S. Production of Bimetallic Carbides by Mechanical Alloying for Catalysis. *Mater. Sci. Forum* **1999**, *299–300*, 121–125. [[CrossRef](#)]
4. Denis, M.C.; Lalande, G.; Guay, D.; Dodelet, J.P.; Schulz, R. High Energy Ball-Milled Pt and Pt-Ru Catalysts for Polymer Electrolyte Fuel Cells and Their Tolerance to CO. *J. Appl. Electrochem.* **1999**, *29*, 951–960. [[CrossRef](#)]
5. Lucariello, M.; Penazzi, N.; Arca, E.; Mulas, G.; Enzo, S. A Structure Investigation of Pt-Co Bimetallic Catalysts Fabricated by Mechanical Alloying. *Mater. Chem. Phys.* **2009**, *114*, 227–234. [[CrossRef](#)]
6. Coutts, J.L.; Devor, R.W.; Aitken, B.; Hampton, M.D.; Quinn, J.W.; Clausen, C.A.; Geiger, C.L. The Use of Mechanical Alloying for the Preparation of Palladized Magnesium Bimetallic Particles for the Remediation of PCBs. *J. Hazard. Mater.* **2011**, *192*, 1380–1387. [[CrossRef](#)] [[PubMed](#)]
7. Zhang, S.S.; Yang, N.; Ni, S.Q.; Natarajan, V.; Ahmad, H.A.; Xu, S.; Fang, X.; Zhan, J. One-Pot Synthesis of Highly Active Ni/Fe Nano-Bimetal by Simultaneous Ball Milling and in Situ Chemical Deposition. *RSC Adv.* **2018**, *8*, 26469–26475. [[CrossRef](#)]
8. Peera, S.G.; Liu, C. Unconventional and Scalable Synthesis of Non-Precious Metal Electrocatalysts for Practical Proton Exchange Membrane and Alkaline Fuel Cells: A Solid-State Co-Ordination Synthesis Approach. *Coord. Chem. Rev.* **2022**, *463*, 214554. [[CrossRef](#)]



9. Kosimov, A.; Alimbekova, A.; Assafrei, J.-M.; Yusibova, G.; Aruväli, J.; Käärik, M.; Leis, J.; Paiste, P.; Ahmadi, M.; Roohi, K.; et al. Template-Assisted Mechanochemistry Leading to Benchmark Energy Efficiency and Sustainability in the Production of Bifunctional Fe–N–C Electrocatalysts. *ACS Sustain. Chem. Eng.* **2023**, *11*, 10825–10834. [[CrossRef](#)]
10. Samriti; Tyagi, R.; Ruzimuradov, O.; Prakash, J. Fabrication Methods and Mechanisms for Designing Highly-Efficient Photocatalysts for Energy and Environmental Applications. *Mater. Chem. Phys.* **2023**, *307*, 128108. [[CrossRef](#)]
11. De Bellis, J.; Petersen, H.; Ternieden, J.; Pfänder, N.; Weidenthaler, C.; Schüth, F. Direct Dry Synthesis of Supported Bimetallic Catalysts: A Study on Comminution and Alloying of Metal Nanoparticles. *Angew. Chem.-Int. Ed.* **2022**, *61*, e202208016. [[CrossRef](#)] [[PubMed](#)]
12. Guzzi, L.; Takács, L.; Stefler, G.; Koppány, Z.; Borkó, L. Re-Co/Al<sub>2</sub>O<sub>3</sub> Bimetallic Catalysts Prepared by Mechanical Treatment: CO Hydrogenation and CH<sub>4</sub> Conversion. *Catal. Today* **2002**, *77*, 237–243. [[CrossRef](#)]
13. Mussio, A.; Danielis, M.; Divins, N.J.; Llorca, J.; Colussi, S.; Trovarelli, A. Structural Evolution of Bimetallic PtPd/CeO<sub>2</sub> Methane Oxidation Catalysts Prepared by Dry Milling. *ACS Appl. Mater. Interfaces* **2021**, *13*, 31614–31623. [[CrossRef](#)]
14. De Bellis, J.; Felderhoff, M.; Schüth, F. Mechanochemical Synthesis of Supported Bimetallic Catalysts. *Chem. Mater.* **2021**, *33*, 2037–2045. [[CrossRef](#)]
15. Zhang, Y.; Li, S.; Yuan, Z.; Chen, H.; Fan, X. Mechanochemical Synthesis of RuCo/MgTiO<sub>3</sub> Catalysts for Nonthermal Plasma-Assisted Ammonia Synthesis. *Ind. Eng. Chem. Res.* **2022**, *61*, 14199–14210. [[CrossRef](#)]
16. Ralphs, K.; Collins, G.; Manyar, H.; James, S.L.; Hardacre, C. Selective Hydrogenation of Stearic Acid Using Mechanochemically Prepared Titania-Supported Pt and Pt-Re Bimetallic Catalysts. *ACS Sustain. Chem. Eng.* **2022**, *10*, 6934–6941. [[CrossRef](#)]
17. da Silva, R.T.P.; Córdoba De Torresi, S.I.; de Oliveira, P.F.M. Mechanochemical Strategies for the Preparation of SiO<sub>2</sub>-Supported AgAu Nanoalloy Catalysts. *Front. Chem.* **2022**, *10*, 1–10. [[CrossRef](#)] [[PubMed](#)]
18. Kley, K.S.; De Bellis, J.; Schüth, F. Selective Hydrogenation of Highly Concentrated Acetylene Streams over Mechanochemically Synthesized PdAg Supported Catalysts. *Catal. Sci. Technol.* **2022**, *13*, 119–131. [[CrossRef](#)]
19. Fazlikeshteli, S.; Vendrell, X.; Llorca, J. Catalytic Partial Oxidation of Methane over Bimetallic Ru–Ni Supported on CeO<sub>2</sub> for Syngas Production. *Int. J. Hydrogen Energy* **2023**, in press. [[CrossRef](#)]
20. Gunnarson, A.; De Bellis, J.; Imhof, T.; Pfänder, N.; Ledendecker, M.; Schüth, F. Facile Solid-State Synthesis of Supported PtNi and PtCo Bimetallic Nanoparticles for the Oxygen Reduction Reaction. *Chem. Mater.* **2023**, *35*, 2006–2015. [[CrossRef](#)]
21. Braga, A.; Armengol-Profítos, M.; Pascua-Solé, L.; Vendrell, X.; Soler, L.; Serrano, I.; Villar-García, I.J.; Pérez-Dieste, V.; Divins, N.J.; Llorca, J. Bimetallic NiFe Nanoparticles Supported on CeO<sub>2</sub> as Catalysts for Methane Steam Reforming. *ACS Appl. Nano Mater.* **2023**, *6*, 7173–7185. [[CrossRef](#)]
22. Wu, T.; Dang, Q.; Wu, Y.; Lei, T.; Yu, J. Catalytic Hydrolysis of Biomass over NiMo Bimetallic Carbon-Based Catalysts. *J. Environ. Chem. Eng.* **2023**, *11*, 110024. [[CrossRef](#)]
23. Mukherjee, P.; Patil, I.; Kakade, B.; Kumar Das, S.; Sahu, A.K.; Swami, A. Methodical Designing of Pt<sub>3–x</sub>Co<sub>0.5+y</sub>Ni<sub>0.5+y</sub>/C (x = 0, 1, 2; y = 0, 0.5, 1) Particles Using a Single-Step Solid State Chemistry Method as Efficient Cathode Catalyst in H<sub>2</sub>-O<sub>2</sub> Fuel Cells. *Catal. Today* **2023**, *423*, 113963. [[CrossRef](#)]
24. Dumitrescu, M.A.; Lucariello, M.; Arca, E.; Manzoli, M.; Francia, C.; Ambrosio, E.P. Nanostructured Bimetallic Alloys Prepared via Mechanochemical Synthesis as PEMFC Electrocatalysts for Automotive Applications. *J. Appl. Electrochem.* **2009**, *39*, 2115–2121. [[CrossRef](#)]
25. Divins, N.J.; Braga, A.; Vendrell, X.; Serrano, I.; Garcia, X.; Soler, L.; Lucentini, I.; Danielis, M.; Mussio, A.; Colussi, S.; et al. Investigation of the Evolution of Pd-Pt Supported on Ceria for Dry and Wet Methane Oxidation. *Nat. Commun.* **2022**, *13*, 5080. [[CrossRef](#)] [[PubMed](#)]
26. Munnik, P.; de Jongh, P.E.; de Jong, K.P. Recent Developments in the Synthesis of Supported Catalysts. *Chem. Rev.* **2015**, *115*, 6687–6718. [[CrossRef](#)] [[PubMed](#)]
27. Hierso, J.-C.; Feurer, R.; Kalck, P. Platinum, Palladium and Rhodium Complexes as Volatile Precursors for Depositing Materials. *Coord. Chem. Rev.* **1998**, *178–180*, 1811–1834. [[CrossRef](#)]
28. Stern, K.H. High Temperature Properties and Decomposition of Inorganic Salts Part 3, Nitrates and Nitrites. *J. Phys. Chem. Ref. Data* **1972**, *1*, 747–772. [[CrossRef](#)]
29. Gallagher, P.K.; Gross, M.E. The Thermal Decomposition of Palladium Acetate. *J. Therm. Anal.* **1986**, *31*, 1231–1241. [[CrossRef](#)]
30. Yuvaraj, S.; Fan-Yuan, L.; Tsong-Huei, C.; Chuin-Tih, Y. Thermal Decomposition of Metal Nitrates in Air and Hydrogen Environments. *J. Phys. Chem. B* **2003**, *107*, 1044–1047. [[CrossRef](#)]
31. Jones, J.; Xiong, H.; DeLaRiva, A.T.; Peterson, E.J.; Pham, H.; Challa, S.R.; Qi, G.; Oh, S.; Wiebenga, M.H.; Pereira Hernandez, X.I.; et al. Thermally Stable Single-Atom Platinum-on-Ceria Catalysts via Atom Trapping. *Science* **2016**, *353*, 150–154. [[CrossRef](#)]
32. Mercado-Zúñiga, C.; Vargas-García, J.R.; Hernández-Pérez, M.A.; Figueroa-Torres, M.Z.; Cervantes-Sodi, F.; Torres-Martínez, L.M. Synthesis of Highly Dispersed Platinum Particles on Carbon Nanotubes by an in Situ Vapor-Phase Method. *J. Alloys Compd.* **2014**, *615*, S538–S541. [[CrossRef](#)]
33. Danielis, M.; Colussi, S.; de Leitenburg, C.; Soler, L.; Llorca, J.; Trovarelli, A. Outstanding Methane Oxidation Performance of Palladium-Embedded Ceria Catalysts Prepared by a One-Step Dry Ball-Milling Method. *Angew. Chem. Int. Ed.* **2018**, *57*, 10212–10216. [[CrossRef](#)] [[PubMed](#)]

34. Danielis, M.; Colussi, S.; de Leitenburg, C.; Trovarelli, A. The Role of Palladium Salt Precursors in Pd-PdO/CeO<sub>2</sub> Catalysts Prepared by Dry Milling for Methane Oxidation. *Catal. Commun.* **2020**, *135*, 105899. [[CrossRef](#)]
35. Pascoli, C. *Bimetallic Methane Oxidation Catalysts Prepared by Dry Methods: Precursors Effect*; Università degli Studi di Udine: Udine, Italy, 2017.
36. Křenek, T.; Kovářík, T.; Pola, M.; Jakubec, I.; Bezdička, P.; Bastl, Z.; Pokorná, D.; Urbanová, M.; Galíková, A.; Pola, J. Enhancement of Thermal Stability of Silver(I) Acetylacetonate by Platinum(II) Acetylacetonate. *Thermochim. Acta* **2013**, *554*, 1–7. [[CrossRef](#)]
37. Sun, H.; Wang, Y.; Xu, S.; Osman, A.I.; Stenning, G.; Han, J.; Sun, S.; Rooney, D.; Williams, P.T.; Wang, F.; et al. Understanding the Interaction between Active Sites and Sorbents during the Integrated Carbon Capture and Utilization Process. *Fuel* **2021**, *286*, 119308. [[CrossRef](#)]
38. Arellano-Treviño, M.A.; Kanani, N.; Jeong-Potter, C.W.; Farrauto, R.J. Bimetallic Catalysts for CO<sub>2</sub> Capture and Hydrogenation at Simulated Flue Gas Conditions. *Chem. Eng. J.* **2019**, *375*, 121953. [[CrossRef](#)]
39. Mussio, A. *Bimetallic Catalysts Prepared by Mechanical Milling for Natural Gas Vehicles Applications*; Università degli Studi di Udine: Udine, Italy, 2021.
40. Mongiat, L. *Bimetallic Catalysts for Natural Gas Fueled Vehicles Methane Abatement*; Università degli Studi di Udine: Udine, Italy, 2015.
41. Shatov, A.V.; Ponomarev, S.S.; Firstov, S.A. 1.09-Hardness and Deformation of Hardmetals at Room Temperature. In *Comprehensive Hard Materials*; Sarin, V.K., Ed.; Elsevier: Oxford, UK, 2014; pp. 267–299. ISBN 978-0-08-096528-4.
42. Bradt, R.C. Ceramic Crystals and Polycrystals, Hardness Of. In *Encyclopedia of Materials: Science and Technology*; Buschow, K.H.J., Cahn, R.W., Flemings, M.C., Ilshner, B., Kramer, E.J., Mahajan, S., Veyssièrè, P., Eds.; Elsevier: Oxford, UK, 2001; pp. 1045–1051. ISBN 978-0-08-043152-9.
43. Wu, Q.; Miao, W.; Zhang, Y.; Gao, H.; Hui, D. Mechanical Properties of Nanomaterials: A Review. *Nanotechnol. Rev.* **2020**, *9*, 259–273. [[CrossRef](#)]
44. Bardini, L.; Pappacena, A.; Dominguez-Escalante, M.; Llorca, J.; Boaro, M.; Trovarelli, A. Structural and Electrocatalytic Properties of Molten Core Sn@SnO<sub>x</sub> Nanoparticles on Ceria. *Appl. Catal. B Environ.* **2016**, *197*, 254–261. [[CrossRef](#)]
45. Feng, X.; Gong, X.; Liu, D.; Li, Y.; Jiang, Y.; Zhang, Y. Bayesian Optimization-Guided Discovery of High-Performance Methane Combustion Catalysts Based on Multi-Component PtPd@CeZrO<sub>x</sub> Core-Shell Nanospheres. *Angew. Chem. Int. Ed.* **2023**, *62*, e202313068. [[CrossRef](#)]
46. Hajji, H.; Nasr, S.; Millot, N.; Salem, E.B. Study of the Effect of Milling Parameters on Mechanochemical Synthesis of Hydroxyfluorapatite Using the Taguchi Method. *Powder Technol.* **2019**, *356*, 566–580. [[CrossRef](#)]
47. Leardi, R. Experimental Design in Chemistry: A Tutorial. *Anal. Chim. Acta* **2009**, *652*, 161–172. [[CrossRef](#)]
48. Czitrom, V. Teacher’s Corner: One-Factor-at-a-Time Versus Designed Experiments. *Am. Stat.* **1999**, *53*, 126–131.
49. Brereton, R.G. *Chemometrics: Data Analysis for the Laboratory and Chemical Plant*; John Wiley & Sons: Hoboken, NJ, USA, 2016; ISBN 0-471-48977-8.
50. Box, G.E.P.; Hunter, J.S.; Hunter, W.G. *Statistics for Experimenters: Design, Innovation, and Discovery*; Wiley, Ed.; Wiley: Hoboken, NJ, USA, 2005; ISBN 978-0-471-71813-0.
51. Yu, W.; Porosoff, M.D.; Chen, J.G. Review of Pt-Based Bimetallic Catalysis: From Model Surfaces to Supported Catalysts. *Chem. Rev.* **2012**, *112*, 5780–5817. [[CrossRef](#)]
52. Miyata, T.; Li, D.; Shiraga, M.; Shishido, T.; Oumi, Y.; Sano, T.; Takehira, K. Promoting Effect of Rh, Pd and Pt Noble Metals to the Ni/Mg(Al)O Catalysts for the DSS-like Operation in CH<sub>4</sub> Steam Reforming. *Appl. Catal. A Gen.* **2006**, *310*, 97–104. [[CrossRef](#)]
53. Jaiswar, V.K.; Katheria, S.; Deo, G.; Kunzru, D. Effect of Pt Doping on Activity and Stability of Ni/MgAl<sub>2</sub>O<sub>4</sub> Catalyst for Steam Reforming of Methane at Ambient and High Pressure Condition. *Int. J. Hydrogen Energy* **2017**, *42*, 18968–18976. [[CrossRef](#)]
54. Schilling, C.; Hofmann, A.; Hess, C.; Ganduglia-Pirovano, M.V. Raman Spectra of Polycrystalline CeO<sub>2</sub>: A Density Functional Theory Study. *J. Phys. Chem. C* **2017**, *121*, 20834–20849. [[CrossRef](#)]
55. Liu, Y.M.; Wang, L.C.; Chen, M.; Xu, J.; Cao, Y.; He, H.Y.; Fan, K.N. Highly Selective Ce-Ni-O Catalysts for Efficient Low Temperature Oxidative Dehydrogenation of Propane. *Catal. Lett.* **2009**, *130*, 350–354. [[CrossRef](#)]
56. Fantozzi, N.; Volle, J.-N.; Porcheddu, A.; Virieux, D.; García, F.; Colacino, E. Green Metrics in Mechanochemistry. *Chem. Soc. Rev.* **2023**, *52*, 6680–6714. [[CrossRef](#)]
57. Ardila-Fierro, K.J.; Hernández, J.G. Sustainability Assessment of Mechanochemistry by Using the Twelve Principles of Green Chemistry. *ChemSusChem* **2021**, *14*, 2145–2162. [[CrossRef](#)]
58. Felderhoff, S.R. Michael On the Theory and Recent Developments in “Batch Mechanochemical Synthesis–Scale-Up”. In *Mechanochemistry and Emerging Technologies for Sustainable Chemical Manufacturing*; CRC Press: Boca Raton, FL, USA, 2023; ISBN 978-1-00-317818-7.
59. Santhanam, P.R.; Dreizin, E.L. Predicting Conditions for Scaled-up Manufacturing of Materials Prepared by Ball Milling. *Powder Technol.* **2012**, *221*, 403–411. [[CrossRef](#)]
60. Mio, H.; Kano, J.; Saito, F. Scale-up Method of Planetary Ball Mill. *Chem. Eng. Sci.* **2004**, *59*, 5909–5916. [[CrossRef](#)]

61. He, X.; Deng, Y.; Zhang, Y.; He, Q.; Xiao, D.; Peng, M.; Zhao, Y.; Zhang, H.; Luo, R.; Gan, T.; et al. Mechanochemical Kilogram-Scale Synthesis of Noble Metal Single-Atom Catalysts. *Cell Rep. Phys. Sci.* **2020**, *1*, 100004. [[CrossRef](#)]
62. Acevedo-Córdoba, L.F.; Vargas-Montañez, O.J.; Velasco-Rozo, E.A.; Mora-Vergara, I.D.; de León, J.N.D.; Pérez-Martínez, D.; Morales-Valencia, E.M.; Baldovino-Medrano, V.G. Mechanochemical Approach for the Preparation of Technical Catalysts. *Catal. Today* **2023**, 114474, in press. [[CrossRef](#)]

**Disclaimer/Publisher's Note:** The statements, opinions and data contained in all publications are solely those of the individual author(s) and contributor(s) and not of MDPI and/or the editor(s). MDPI and/or the editor(s) disclaim responsibility for any injury to people or property resulting from any ideas, methods, instructions or products referred to in the content.